Chemical Engineering Journal 157 (2010) 509–519

Contents lists available at ScienceDirect

Chemical Engineering Journal

journal homepage: www.elsevier.com/locate/cej

Relationship between flow structure and transfer coefficients in fast fluidized beds

Baolin Hou [a,b], Hongzhong Li [a,*]

[a] State Key Laboratory of Multi-phase Complex Systems, Institute of Process Engineering, Chinese Academy of Sciences, P.O. Box 353, Beijing 100190, PR China
[b] Graduate School of Chinese Academy of Science, Beijing 100049, PR China

ARTICLE INFO

Article history:
Received 21 August 2009
Received in revised form
24 December 2009
Accepted 29 December 2009

Keywords:
Structure
Momentum transfer
Mass transfer
Heat transfer
Fast fluidized bed
Multiphase flow
Particle

ABSTRACT

In this paper, the relationships between the bed structural parameters and momentum transfer, mass transfer and heat transfer in fast fluidized beds are analyzed for Geldart A or B particles. The influence of dispersion and aggregation of particles on the mass transfer coefficient and heat transfer coefficient is discussed. The equations for calculating the drag force coefficient, mass transfer coefficient and heat transfer coefficient in fast fluidized beds are developed based on eight structural parameters (U_{fd}, U_{fc}, U_{pd}, U_{pc}, d_c, f, ε_d and ε_c) of heterogeneous beds, which can be solved by the Energy-Minimization Multi-Scale (EMMS) model. The drag force has been calculated based on the local bed structural parameters and the calculated solids flux and solids concentration are compared with the experimental data in the literature. For the heat transfer and mass transfer, the averaged bed structural parameters are employed to calculate the averaged heat transfer and mass transfer coefficients, and the results are compared with the experimental data from the literature. The simulating results are in good agreement with experimental data.

1. Introduction

It is well established [1,2] that a fast fluidized bed is non-uniform in radial and axial solids distributions. Axially the existence of two regions results in an S-shaped voidage profile, and radially the solids concentration is low at the center but dense near the wall. Moreover, the particles distribution is also non-uniform on a sub-bed scale and many particle clusters are distributed in dispersed particles. The clusters are subjected to dynamic processes of aggregation and destruction due to both fluid-particle and particle–particle interactions, and the shape and size of clusters change constantly. Furthermore, the particles velocity are higher in the center of the bed but lower near the wall and higher in the dispersed phase but lower in the cluster phase; while the gas velocity is higher at the bed center but lower near the wall, and it is higher in the dispersed phase but lower in the cluster phase. It is obvious that in fast fluidized beds there exist heterogeneous structures on both macro-scale and meso-scale.

Both experimental results and theoretical analysis indicate that the bed structures show significant effects on the momentum transfer behavior. According to Yang et al. [3], under the same superficial gas velocity, superficial particle velocity and averaged voidage, the drag coefficient of particles in gas is 18.6 in the homogeneous fluidized bed, while it decreased to 2.85 in a heterogeneously fluidized bed. Just like the momentum transfer, the influence of the cluster on mass transfer and heat transfer has been reported [4–6], but the theoretical analysis about the influence of flow structure on momentum, mass and heat transfer coefficients is not found in the literature. In the present work, a theoretical analysis on the relationships between local bed structure and momentum, mass and heat transfer coefficients is given. The theoretical prediction was compared with the experiment data in the literature. The prediction results are in good agreement with experimental data.

2. Quantitative description of local structure and gas–particles interaction in fast fluidized bed

Based on the Energy-Minimization Multi-Scale (EMMS) [7], to quantitatively describe the local bed structure of a fast fluidized bed with Geldart A or B particles, eight parameters are needed. They are voidages in dispersed and cluster phases ε_d and ε_c, respectively, superficial gas velocities in dispersed and cluster phases U_{fd} and U_{fc}, respectively, superficial particle velocities in dispersed and cluster phases U_{pd} and U_{pc}, respectively, diameter of cluster d_c, volume fraction of cluster phase f, which can be predicted by using the Energy-Minimization Multi-Scale (EMMS) [7] model when the superficial gas velocity U_f, superficial particle velocity U_p, gas den-

* Corresponding author. Tel.: +86 10 62556951; fax: +86 10 62536108.
E-mail address: hzli@home.ipe.ac.cn (H. Li).

1385-8947/$ – see front matter © 2010 Elsevier B.V. All rights reserved.
doi:10.1016/j.cej.2009.12.047

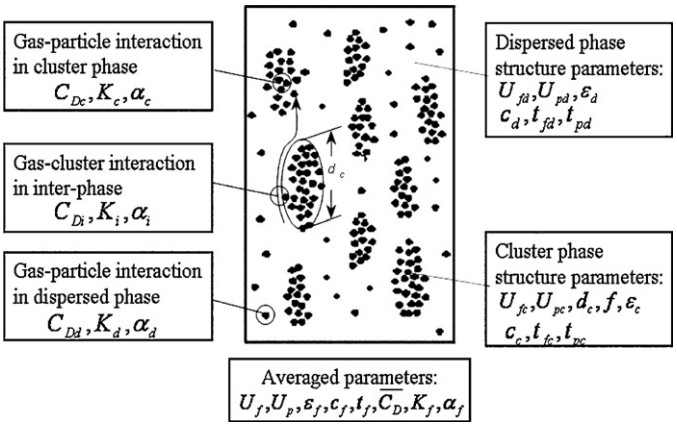

Fig. 1. Resolution of structure and gas–particles interaction in fast fluidized bed.

sity ρ_f, gas viscosity μ_f, particle density ρ_p, and particle diameter d_p are given [7]. However, the difference between the particles inside cluster and the particles on the surface of the cluster is not considered in the literature [7]. The particles on the surface of cluster contact with flowing gas in the dispersed phase, these particles are different from the particles inside cluster. Thus, the equivalent number of particles should be subtracted from the total number of particles in a cluster, which is expressed by a coefficient $(1-2d_p/d_c)$. So the equation for the drag force exerted on particles in cluster by flowing gas is revised as:

$$\left(1-2\frac{d_p}{d_c}\right)\frac{f(1-\varepsilon_c)}{(\pi/6)d_p^3}C_{dc}\frac{1}{2}\rho_f U_{sc}^2\frac{\pi}{4}d_p^2 = f(\rho_p-\rho_f)g(1-\varepsilon_f) \quad (1)$$

The resolution of structure and gas–particles interaction in fast fluidized bed is shown in Fig. 1. It shows that if mass transfer and heat transfer are to be estimated, additional parameters are necessary. They are the component concentrations of gas in dispersed and cluster phases, c_d and c_c, the temperatures of gas in dispersed and cluster phases, t_{fd} and t_{fc}, the temperatures of particles in dispersed and cluster phases, t_{pd} and t_{pc}. They can be solved by using the mass conservation equation and heat conservation equation for dispersed and cluster phases. The parameters for gas–particles interaction, i.e., drag coefficient C_D, mass transfer coefficient K_f, and heat transfer coefficient α_f, are the functions of structure parameters.

3. Drag coefficient C_D

Yang et al. [3] proposed a resolution for the relationship between drag coefficient and bed structure in circulating fluidized bed. Based on that work [3], a theoretical analysis on the relationship between drag coefficient and bed structure in fast fluidized beds is conducted in the present work, and attention is paid to the particles on the surface of clusters, because the environment of the particles on the cluster surface is different from that both inside and outside clusters. Furthermore, the distributions of particles in dispersed phase and cluster phase and the distribution of clusters enmeshed in dispersed phase are all treated as homogeneous.

3.1. Drag force of flowing gas on single particle in dispersed phase F_{Dd}

In general, the voidage in dispersed phase is larger than 0.8, i.e., $\varepsilon_d > 0.8$ so that the drag coefficient C_{Dd} can been obtained by using Wen–Yu's equation [8] as follows:

$$C_{Dd} = C_{D0}\varepsilon_d^{-4.7} \quad \text{for } \varepsilon_f > 0.8 \quad (2)$$

where C_{D0} is the drag coefficient for single particles in gas flow, and

$$C_{D0} = 0.44 \quad \text{for } Re_p > 1000 \quad (3)$$

$$C_{D0} = \frac{24}{Re_p}(1+0.15Re_p^{0.687}) \quad \text{for } Re_p < 1000 \quad (4)$$

Re_p is the Reynolds Number of particle:

$$Re_p = \frac{\rho_f d_p(u_f-u_p)\varepsilon_f}{\mu_f} \quad (5)$$

and

$$F_{Dd} = C_{Dd}\rho_f\frac{1}{2}|U_{sd}|U_{sd}\frac{\pi}{4}d_p^2 \quad (6)$$

where U_{sd} is the superficial slip velocity between gas and particle in the dispersed phase:

$$U_{sd} = U_{fd} - U_{pd}\frac{\varepsilon_d}{1-\varepsilon_d} \quad (7)$$

3.2. Drag force of flowing gas on single particle in cluster phase F_{Dc}

In general, the voidage in cluster phase is less than 0.8, i.e., $\varepsilon_c < 0.8$, so that the drag coefficient C_{Dc} can been obtained by changing the form of Ergun's equation [9] as follows.

The drag force of gas flow on particles in the unit volume of cluster phase, F_{Dcu}, can been calculated by

$$\begin{aligned} F_{Dcu} &= 150\frac{(1-\varepsilon_c)^2\mu_f}{\varepsilon_c^3 d_p^2}U_{sc} + 1.75\frac{(1-\varepsilon_c)\rho_f}{\varepsilon_c^3 d_p}|U_{sc}|U_{sc} \\ &= \left[300\frac{4(1-\varepsilon_c)^2\mu_f}{\pi\varepsilon_c^3\rho_f d_p^4 U_{sc}} + \frac{7(1-\varepsilon_c)}{3\pi\varepsilon_c^3 d_p^3}\right]\frac{1}{2}\rho_f|U_{sc}|U_{sc}\frac{\pi}{4}d_p^2\frac{(1-\varepsilon_c)(\pi/6)d_p^3}{(1-\varepsilon_c)(\pi/6)d_p^3} \\ &= \left[200\frac{(1-\varepsilon_c)\mu_f}{\varepsilon_c^3\rho_f d_p U_{sc}} + \frac{7}{3\varepsilon_c^3}\right]\frac{1}{2}\rho_f|U_{sc}|U_{sc}\frac{\pi}{4}d_p^2\frac{1-\varepsilon_c}{(\pi/6)d_p^3} \end{aligned} \quad (8)$$

where $(1-\varepsilon_c)/(\pi/6)d_p^3$ is the expression of the number of particles in the unit volume of cluster phase.

By comparing Eq. (8) with Eq. (6), the drag coefficient C_{Dc} should be

$$C_{Dc} = 200\frac{(1-\varepsilon_c)\mu_f}{\varepsilon_c^3\rho_f d_p U_{sc}} + \frac{7}{3\varepsilon_c^3} \quad (9)$$

and the drag force on single particles in cluster phase F_{Dc} is

$$F_{Dc} = C_{Dc}\frac{1}{2}\rho_f|U_{sc}|U_{sc}\frac{\pi}{4}d_p^2 \quad (10)$$

where U_{sc} is the superficial slip velocity between gas and particles in cluster phase, namely

$$U_{sc} = U_{fc} - U_{pc}\frac{\varepsilon_c}{1-\varepsilon_c} \quad (11)$$

3.3. Drag force of flowing gas in dispersed phase on single cluster F_{Di}

The single cluster can be treated as a big particle with the equivalent diameter d_c. In analogy with Eqs. (6), (2) and (9), we have

$$F_{Di} = C_{Di}\frac{1}{2}\rho_f|U_{si}|U_{si}\frac{\pi}{4}d_c^2 \quad (12)$$

where C_{Di} is the drag coefficient of a cluster in gas of dispersed phase, and

$$C_{Di} = C_{D0}\varepsilon_i^{-4.7} \quad \text{for } \varepsilon_i > 0.8 \tag{13}$$

$$C_{Di} = 200\frac{(1-\varepsilon_i)\mu_f}{\varepsilon_i^3 \rho_f d_c U_{si}} + \frac{7}{3\varepsilon_i^3} \quad \text{for } \varepsilon_i < 0.8 \tag{14}$$

ε_i is the voidage of the inter-phase, i.e., the volume fraction of gas which does not include gas in clusters:

$$\varepsilon_i = \varepsilon_d(1-f) \tag{15}$$

U_{si} is the superficial slip velocity between gas in dispersed phase and cluster:

$$U_{si} = \left[U_{fd} - U_{pc}\frac{\varepsilon_d}{1-\varepsilon_c}\right](1-f) = \left[\frac{U_{fd}}{\varepsilon_d} - \frac{U_{pc}}{1-\varepsilon_c}\right]\varepsilon_d(1-f) \tag{16}$$

3.4. Drag force of flowing gas in cluster phase on particles in cluster F_{Dcn}

F_{Dcn} can be obtained by multiplying F_{Dc} by the particles number in a cluster. Because the particles on the cluster surface contact with flowing gas in the dispersed phase, the equivalent number of particles, whose surface area is equal to the contact area between cluster surface particles and gas in the dispersed phase, should be subtracted from the total number of particles in a cluster. Thus we have

$$\begin{aligned} F_{Dcn} &= \left[\frac{(\pi/6)d_c^3(1-\varepsilon_c)}{(\pi/6)d_p^3} - \frac{\pi d_c^2(1-\varepsilon_c)}{(2/4)\pi d_p^2}\right]F_{Dc} \\ &= (1-\varepsilon_c)\left[\left(\frac{d_c}{d_p}\right)^3 - 2\left(\frac{d_c}{d_p}\right)^2\right]F_{Dc} \end{aligned} \tag{17}$$

3.5. Total drag force of gas on particles in a unit volume of gas–particles flow F_D

The total drag force is the sum of the drag force on the particles in dispersed phase, that on the particles in cluster phase, and the drag on the cluster surface, that is

$$\begin{aligned} F_D &= \frac{(1-f)(1-\varepsilon_d)}{(\pi/6)d_p^3}F_{Dd} + \frac{f}{(\pi/6)d_c^3}F_{Dcn} + \frac{f}{(\pi/6)d_c^3}F_{Di} \\ &= \frac{(1-f)(1-\varepsilon_d)}{(\pi/6)d_p^3}C_{Dd}\frac{1}{2}\rho_f|U_{sd}|U_{sd}\frac{\pi}{4}d_\rho^2 \\ &\quad + (1-2(d_p/d_c))\frac{f(1-\varepsilon_c)}{(\pi/6)d_p^3}C_{Dc}\frac{1}{2}\rho_f|U_{sc}|U_{sc}\frac{\pi}{4}d_p^2 \\ &\quad + \frac{f}{(\pi/6)d_c^3}C_{Di}\frac{1}{2}\rho_f|U_{si}|U_{si}\frac{\pi}{4}d_c^2 \end{aligned} \tag{18}$$

3.6. Averaged drag coefficient $\overline{C_D}$

According to the definition of averaged drag coefficient, the drag force can be calculated by

$$F_D = \frac{1-\varepsilon_f}{(\pi/6)d_p^3}\overline{C_D}\frac{1}{2}\rho_f|U_s|U_s\frac{\pi}{4}d_p^2 \tag{19}$$

where ε_f is the averaged voidage, and U_s is the superficial slip velocity between gas and particles, respectively:

$$\varepsilon_f = \varepsilon_c f + (1-f)\varepsilon_d \tag{20}$$

$$U_s = U_f - U_p\frac{\varepsilon_f}{1-\varepsilon_f} \tag{21}$$

The equation for averaged drag coefficient $\overline{C_D}$ can be obtained by comparing Eq. (19) with Eq. (18):

$$\overline{C_D} = \frac{\begin{array}{c} f(1-\varepsilon_c)(1-2(d_p/d_c))C_{Dc}|U_{sc}|U_{sc} + (1-f) \\ \times(1-\varepsilon_d)C_{Dd}|U_{sd}|U_{sd} + f(d_p/d_c)C_{Di}|U_{si}|U_{si} \end{array}}{(1-\varepsilon_f)|U_s|U_s} \tag{22}$$

In contrast, the traditional equation for $\overline{C_D}$ is

$$\overline{C_D} = C_{D0}\varepsilon_f^{-4.7} \tag{23}$$

It can be seen that Eq. (22) is very different from Eq. (23). The former is affected by many structure parameters and essentially a weighted average of C_D in different phases.

4. Coefficient of mass transfer K_f

4.1. Coefficient of mass transfer between gas and particles in homogeneous gas–particles system

In this case, the Jung–La Nauze's equation [10] is recommended as:

$$Sh = 2\varepsilon + 0.69\left(\frac{U_s d_p \rho_f}{\varepsilon\mu_f}\right)^{1/2} Sc^{1/3} \tag{24}$$

where Sh is the Sherwood number, Sc is the Schmidt number, and ε is the voidage, and

$$Sh = \frac{Kd_p}{D} \tag{25}$$

$$Sc = \frac{\mu_f}{\rho_f D} \tag{26}$$

where D is the gas diffusion coefficient. Substituting Eqs. (25) and (26) into Eq. (24) yields:

$$K = Sh\frac{D}{d_p} = 2\varepsilon\frac{D}{d_p} + 0.69\frac{D}{d_p}\left(\frac{U_s d_p \rho_f}{\varepsilon\mu_f}\right)^{1/2}\left(\frac{\mu_f}{\rho_f D}\right)^{1/3} \tag{27}$$

4.2. Coefficients of mass transfer between gas and particles in heterogeneous gas–particles system

The heterogeneous gas–particles system consists of dispersed and cluster phases. The distribution of particles in both phases and the distribution of clusters in this system can be taken as homogeneous. Therefore, the coefficient of mass transfer between gas and particles in dispersed phase K_d, that between gas and particles in cluster phase K_c, and that between cluster and gas in dispersed phase K_i can be given by analogy with Eq. (27):

$$K_d = 2\varepsilon_d\frac{D}{d_p} + 0.69\frac{D}{d_p}\left(\frac{U_{sd} d_p \rho_f}{\varepsilon_d\mu_f}\right)^{1/2}\left(\frac{\mu_f}{\rho_f D}\right)^{1/3} \tag{28}$$

$$K_c = 2\varepsilon_c\frac{D}{d_p} + 0.69\frac{D}{d_p}\left(\frac{U_{sc} d_p \rho_f}{\varepsilon_c\mu_f}\right)^{1/2}\left(\frac{\mu_f}{\rho_f D}\right)^{1/3} \tag{29}$$

$$K_i = 2\varepsilon_d(1-f)\frac{D}{d_c} + 0.69\frac{D}{d_c}\left(\frac{U_{si} d_c \rho_f}{\varepsilon_d(1-f)\mu_f}\right)^{1/2}\left(\frac{\mu_f}{\rho_f D}\right)^{1/3} \tag{30}$$

4.3. Mass transfer between gas and particles in heterogeneous gas–particles system

An air and naphthalene particles system is used to illustrate our approach to estimation of the mass transfer coefficient.

The naphthalene particles continuously release naphthalene into the air by sublimation. The mass of naphthalene transferred from the particles into air flow in unit volume of the system M consists of four parts:

$$M = M_d + M_c + M_i + M_a \tag{31}$$

in which M_d transferred from particles to air in the same dispersed phase, M_c transferred from particles to air in the same cluster phase, M_i transferred from particles on the cluster surface to air in the dispersed phase, and M_a transferred from particles to air due to aggregating and dispersing of the particles.

According to the principle of mass transfer [11], M_d, M_c and M_i can be expressed respectively as

$$M_d = K_d a_p(1-\varepsilon_d)(1-f)(c_s - c_d) \tag{32}$$

$$\begin{aligned} M_c &= K_c[a_p(1-\varepsilon_c)f - a_c(1-\varepsilon_c)f](c_s - c_c) \\ &= K_c(a_p - a_c)(1-\varepsilon_c)f(c_s - c_c) \end{aligned} \tag{33}$$

$$M_i = K_i a_c(1-\varepsilon_c)f(c_s - c_d) \tag{34}$$

where a_p is the specific surface area of particle, and $a_p = 6/d_p$ for spherical particle; a_c is the specific surface area of cluster, and $a_c = 6/d_c$ for spherical cluster; c_s, c_d, c_c are the concentrations of naphthalene in air on the surface of particle, in air of the dispersed phase, and in air of the cluster phase, respectively.

It must be noted that when the interfacial area between gas and particles in cluster phase is calculated, the contact area between the particles on the surface of cluster and gas in dispersed phase should be excluded as shown in Eq. (33).

Substituting Eqs. (32)–(34) into Eq. (31) yields

$$\begin{aligned} M &= K_d a_p(1-\varepsilon_d)(1-f)(c_s - c_d) + K_c(a_p - a_c)(1-\varepsilon_c)f(c_s - c_c) \\ &\quad + K_i a_c(1-\varepsilon_c)f(c_s - c_d) + M_a \end{aligned} \tag{35}$$

4.4. Averaged coefficient of mass transfer $\overline{K_f}$

Using averaged mass transfer coefficient, the mass transfer equation is:

$$M = \overline{K_f} a_p(1-\varepsilon_f)(c_s - c_f) \tag{36}$$

where c_f is the averaged concentration of naphthalene in air:

$$c_f \varepsilon_f = c_d \varepsilon_d (1-f) + c_c f \varepsilon_c \tag{37}$$

Combining Eqs. (35) and (36) leads to the equation for averaged mass transfer coefficient:

$$\overline{K_f} = \frac{\begin{array}{l} K_d a_p(1-\varepsilon_d)(1-f)(c_s - c_d) + K_c(a_p - a_c) \\ \times(1-\varepsilon_c)f(c_s - c_c) + K_i a_c(1-\varepsilon_c)f(c_s - c_d) + M_a \end{array}}{a_p(1-\varepsilon_f)(c_s - c_f)} \tag{38}$$

in contrast to the traditional equation for averaged mass transfer coefficient:

$$\overline{K_f} = 2\varepsilon_f \frac{D}{d_p} + 0.69 \frac{D}{d_p}\left(\frac{U_s d_p \rho_f}{\varepsilon_f \mu_f}\right)^{1/2}\left(\frac{\mu_f}{\rho_f D}\right)^{1/3} \tag{39}$$

It can be seen that Eq. (38) is essentially the weighted average of mass transfer coefficient in different regions.

5. Coefficient of heat transfer α_f

5.1. Coefficient of heat transfer between gas and particles in homogeneous gas–particles system α

According to Rowe et al. [12], an equation for heat transfer coefficient, which is similar to the Jung–La Nauze's mass transfer coefficient equation [6], is suggested as follows:

$$Nu = 2\varepsilon + 0.69\left(\frac{U_s d_p \rho_f}{\varepsilon \mu_f}\right)^{1/2} \mathrm{Pr}^{1/3} \tag{40}$$

where Nu is the Nusselt number, Pr is the Prandtl number as defined respectively by

$$Nu = \frac{\alpha d_p}{\lambda} \tag{41}$$

$$\mathrm{Pr} = \frac{C_p \mu_f}{\lambda} \tag{42}$$

In Eqs. (41) and (42) λ is the heat conductivity of gas, and C_p is the heat capacitivity of gas. Combining Eqs. (40)–(42) yields

$$\alpha = 2\varepsilon \frac{\lambda}{d_p} + 0.69 \frac{\lambda}{d_p}\left(\frac{U_s d_p \rho_f}{\varepsilon \mu_f}\right)^{1/2}\left(\frac{C_p \mu_f}{\lambda}\right)^{1/3} \tag{43}$$

5.2. Coefficients of heat transfer between gas and particles in dispersed phase, in cluster phase, and interface for heterogeneous gas–particles system

The heterogeneous gas–particles system consists of dispersed phase and cluster phase. The distribution of particles in both phases and the distribution of clusters in this system can be treated as homogeneous distribution. Therefore the coefficient of heat transfer between gas and particles in dispersed phase α_d, the coefficient of heat transfer between gas and particles in cluster phase α_c, and the coefficient of heat transfer between cluster and gas in dispersed phase α_i can be given by analogizing with Eq. (43). They are

$$\alpha_d = 2\varepsilon_d \frac{\lambda}{d_p} + 0.69 \frac{\lambda}{d_p}\left(\frac{U_{sd} d_p \rho_f}{\varepsilon_d \mu_f}\right)^{1/2}\left(\frac{C_p \mu_f}{\lambda}\right)^{1/3} \tag{44}$$

$$\alpha_c = 2\varepsilon_c \frac{\lambda}{d_p} + 0.69 \frac{\lambda}{d_p}\left(\frac{U_{sc} d_p \rho_f}{\varepsilon_c \mu_f}\right)^{1/2}\left(\frac{C_p \mu_f}{\lambda}\right)^{1/3} \tag{45}$$

$$\alpha_i = 2\varepsilon_d(1-f) \frac{\lambda}{d_p} + 0.69 \frac{\lambda}{d_c}\left(\frac{U_{si} d_c \rho_f}{\varepsilon_d(1-f)\mu_f}\right)^{1/2}\left(\frac{C_p \mu_f}{\lambda}\right)^{1/3} \tag{46}$$

5.3. Heat transfer between gas and particles in heterogeneous gas–particles system

At present a cold gas and hot particles system is used to illustrate the heat transfer.

The cold gas passes through a fast fluidized bed of hot particles. The heat quantity H transferred from particles to gas in unit volume of the system consists of four parts:

$$H = H_d + H_c + H_i + H_a \tag{47}$$

In which H_d is the heat quantity transferred from particles in dispersed phase to gas in dispersed phase, H_c is heat transferred from particles in cluster phase to gas in cluster phase, H_i that from particles on the surface of cluster to gas in dispersed phase, and H_a being the heat transferred from particles to gas due to aggregation and dispersion of the particles.

According to the principle of heat transfer [11], H_d, H_c and H_i can be expressed as:

$$H_d = \alpha_d a_p (1-\varepsilon_d)(1-f)(t_{pd} - t_{fd}) \quad (48)$$

$$H_c = \alpha_c (a_p - a_c)(1-\varepsilon_c) f (t_{pc} - t_{fc}) \quad (49)$$

$$H_i = \alpha_i a_c (1-\varepsilon_c) f (t_{pc} - t_{fd}) \quad (50)$$

where t_{pd}, t_{pc}, t_{fd}, t_{fc}, are the temperatures of particles in dispersed phase and in cluster phase, the temperatures of gas in dispersed phase and in cluster phase, respectively.

It needs to be noted that when the interfacial heat transfer area between gas and particles in cluster phase is calculated, the contact area between the particles on the surface of cluster and gas in dispersed phase should be subtracted as shown in Eq. (49). Substituting Eqs. (48)–(50) into Eq. (47) yields

$$H = \alpha_d a_p (1-\varepsilon_d)(1-f)(t_{pd} - t_{fd}) + \alpha_c (a_p - a_c)(1-\varepsilon_c) f (t_{pc} - t_{fc}) + \alpha_i a_c (1-\varepsilon_c) f (t_{pc} - t_{fd}) + H_a \quad (51)$$

5.4. Averaged coefficient of heat transfer $\overline{\alpha_f}$

The averaged coefficient of heat transfer is defined as:

$$H = \overline{\alpha_f} a_p (1-\varepsilon_f)(t_p - t_f) \quad (52)$$

where t_p, t_f are the average temperatures of particles and gas, respectively, and they are defined by

$$(1-\varepsilon_f) t_p = (1-f)(1-\varepsilon_d) t_{pd} + f(1-\varepsilon_c) t_{pc} \quad (53)$$

$$\varepsilon_f t_f = (1-f)\varepsilon_d t_{fd} + f \varepsilon_c t_{fc} \quad (54)$$

From Eqs. (51) and (52) it follows:

$$\overline{\alpha_f} = \frac{\alpha_d a_p (1-\varepsilon_d)(1-f)(t_{pd} - t_{fd}) + \alpha_c (a_p - a_c) \times (1-\varepsilon_c) f (t_{pc} - t_{fc}) + \alpha_i a_c (1-\varepsilon_c) f (t_{pc} - t_{fd}) + H_a}{a_p (1-\varepsilon_f)(t_p - t_f)} \quad (55)$$

while the traditional equation for average coefficient of heat transfer is:

$$\overline{\alpha_f} = 2\varepsilon_f \frac{\lambda}{d_p} + 0.69 \frac{\lambda}{d_p} \left(\frac{U_s d_p \rho_f}{\varepsilon_f \mu_f} \right)^{1/2} \left(\frac{C_p \mu_f}{\lambda} \right)^{1/3} \quad (56)$$

It can be seen that Eq. (55) is very different from Eq. (56). The averaged coefficient of heat transfer $\overline{\alpha_f}$ is affected by many parameters of structure for the heterogeneous gas–particles flow system rather than by averaged voidage ε_f and the superficial slip velocity U_s only.

6. Effect of aggregating and dispersing of particles on mass and heat transfer

There are two cases for the cluster aggregating and dispersing. One case is that a single particle is striped from the surface of a cluster, or adhered to the surface of the cluster. During the process of stripping, the slip velocity between gas and single particle decreases due to terminal velocity of the cluster larger than that of single particle, which results in a decrease of mass and heat transfer coefficients. While during the process of adhering, the slip velocity between gas and single particle increases, resulting in an increase of mass and heat transfer coefficients. At the steady condition, the stripping rate equals to the adhering rate, and the negative and positive effects are compensated. Therefore, the effects of stripping and adhering on the mass and heat transfer can be neglected.

Another case is that a big cluster breaks into several small clusters, or several small clusters are aggregated into a big cluster. During the process of breaking, the slip velocity between gas and small cluster decreases due to the terminal velocity of the big cluster larger than that of small cluster, which results in a decrease of mass and heat transfer coefficients. While during the process of aggregating, the slip velocity between gas and small cluster increases resulting in an increase of mass and heat transfer coefficients. At the stable condition the breakup rate equals to the aggregation rate, therefore the effects of breaking and aggregating on the mass and heat transfer coefficients can also be neglected.

7. Model validation

In order to verify the theoretical relationships between the structure and momentum, mass, and heat transfer coefficients developed in this work, the different experiments are employed to check the models by comparing the model predictions with the experimental data in the literature.

7.1. Momentum transfer

The momentum transfer depending on the bed structure, which was firstly evidenced by Yang et al. [3] by employing the Energy-Minimization Multi-Scale (EMMS) method, has been validated with experimental data [7]. Since the difference of gas–particle contact condition between the particles inside cluster and the particles on the surface of cluster was not considered in Yang et al.'s model [3], the momentum conservation equation for cluster phase is revised in this work as follows:

$$\left(1 - 2\frac{d_p}{d_c}\right) \frac{f(1-\varepsilon_c)}{(\pi/6) d_p^3} C_{dc} \frac{1}{2} \rho_f U_{sc}^2 \frac{\pi}{4} d_p^2 + \frac{3}{4} C_{Di} \frac{f}{d_c} \rho_f U_{si}^2 = f(\rho_p - \rho_f)(g + a)(1-\varepsilon_f) \quad (57)$$

It can be seen from Eq. (57) that a coefficient $(1 - 2d_p/d_c)$ is sued to revise the Yong et al.'s momentum conservation equation for cluster phase. And other equations used are the same as used by Yang et al. [3]. In this work, the local eight bed structure parameters are firstly solved by Yang et al.'s EMMS model [3] based on the local averaged gas and solid velocity and voidage. Then, the local drag force between gas and solid can be obtained by Eq. (18), and finally the exchange coefficient of momentum can be calculated by the following equation:

$$\beta_0 = \frac{\varepsilon_f^2}{|U_f - U_p|} F_D \quad (58)$$

On the basis of Eq. (58), the 2D Eurelian approach can be used to simulate the experimental case from Li and Kwauk [7] as Yang et al. did in the literature [3], the simulating process and the method of solution have been described in detail in Appendix A.

Fig. 2 gives a comparison between the experimental data and the simulation results based on the Gidaspow et al. [13] drag model and the drag model developed in this work. From Fig. 2, it can be seen that the simulation based on the model in this work is much closer to the experimental data than the Gidaspow model. Due to the general existence of clusters in fast fluidized beds, these clusters greatly reduce the interaction between gas and solids. The drag model based on the bed structure parameters in this work considers this reduction, so that better prediction of solid flux is obtained.

Fig. 3 gives the comparison of the time-averaged (10 s) axial profiles of voidages between the experimental data and the simulating results based on the different drag models. It is obvious that the present drag model based on the bed structure captures well the coexistence of a dense bottom and dilute top, as well as the S-shaped distribution of particle fraction in axial direction.

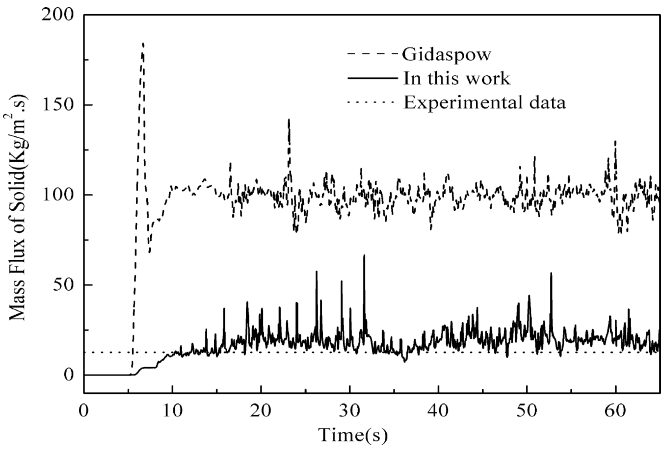

Fig. 2. Computed solids flux near the outlet (U_{g0} = 1.52 m/s, G_s = 14.3 kg/m^2 s, H_0 = 1.25 m).

7.2. Mass transfer

In order to test and validate the developed mass transfer theory in this work, the experimental data reported by Subbarao and Gambhir [14] is used here. In that experiment, under the environmental condition the air saturated with naphthalene is employed to fluidize sand in a glass fast fluidized bed of 105 cm in height and 2.5 cm I.D. The process of the naphthalene adsorbed by sand was thought to be controlled by mass transfer in that experiment. The mass transfer coefficient can be obtained by measuring the increasing weight of sand. Other conditions of experiment and the method of solving have been described in detail in Appendix B. Figs. 4 through 9 show the comparisons of experimental data with the theoretical prediction for the effect of particle diameter and the superficial gas velocity on the average coefficient of mass transfer. These figures demonstrate that the present simulation results of mass transfer coefficient based on multi-scale structure are distinctly better than that based on the traditional average method. Breault and Guenther [15] calculated the mass transfer in fast fluidized bed by replacing the parameters of single particle with the parameters of cluster by a statistical approach in the equation of mass transfer coefficient. Their results are also in good agreement with experimental data, but it is well known that the mass transfer in fast fluidized bed is controlled by both the dispersed and cluster phases, and using the parameters of cluster phase only to characterize the mass transfer in fast fluidized bed is not appropriate.

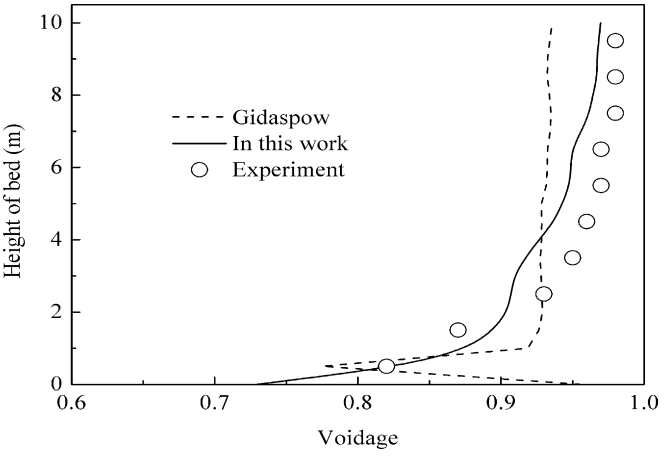

Fig. 3. Comparison between experimental data and simulating results of axial voidage profile.

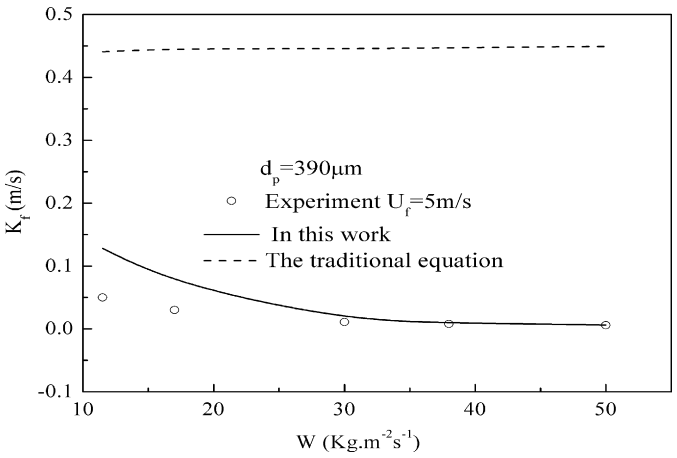

Fig. 4. Comparison of Subbarao's experimental data with theoretical predictions.

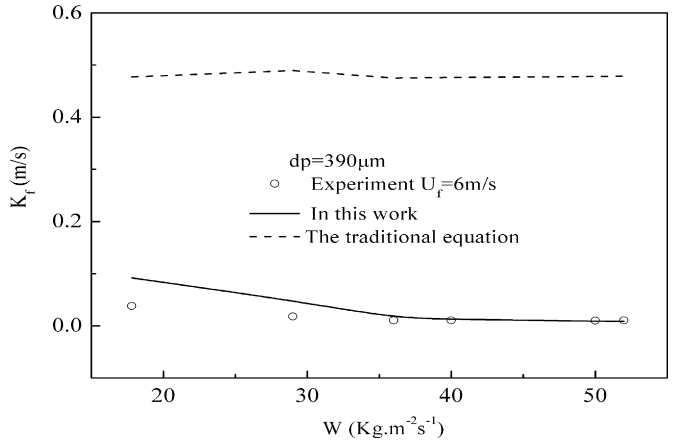

Fig. 5. Comparison of Subbarao's experimental data with theoretical predictions.

The deviation of the simulation results of the mass transfer coefficient based on the traditional average method from experimental data is more than an order of magnitude. The reason is mainly the heterogeneous multi-scale structure in the fast fluidized bed. The influence factors are not only the mass transfer between gas and solids in each phase, but also the gas exchange between dispersed phase and dense phase, as recently reported by Yang et al. [16]. So the mass transfer in the fast fluidized bed is not only the function of mass transfer coefficient in every phase but also the function

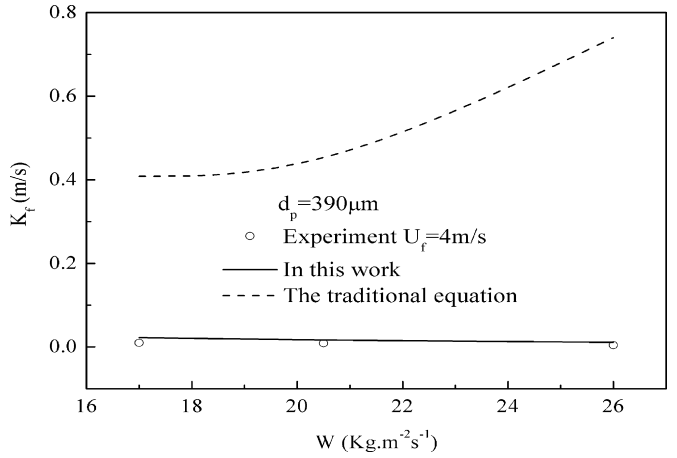

Fig. 6. Comparison of Subbarao's experimental data with theoretical predictions.

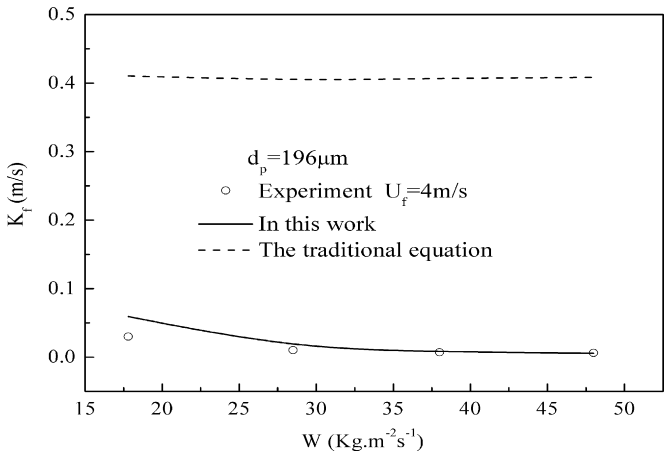

Fig. 7. Comparison of Subbarao's experimental data with theoretical predictions.

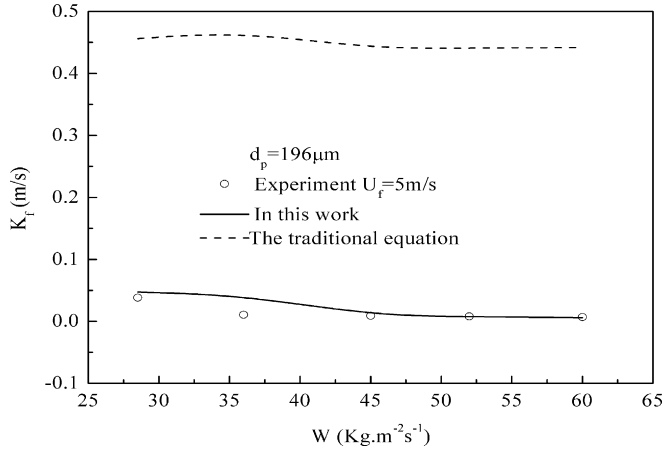

Fig. 8. Comparison of Subbarao's experimental data with theoretical predictions.

of gas component concentration in every phase. This kind of complex influence of cluster on mass transfer in the fast fluidized bed leads to the mass transfer coefficients differ up to seven orders of magnitude in the literature [17,18]. Therefore, only using the traditional average method to accurately calculate this kind of complex process is impossible. The way based on the heterogeneous multiscale structure in this work can more accurately predict the mass transfer in the fast fluidized bed.

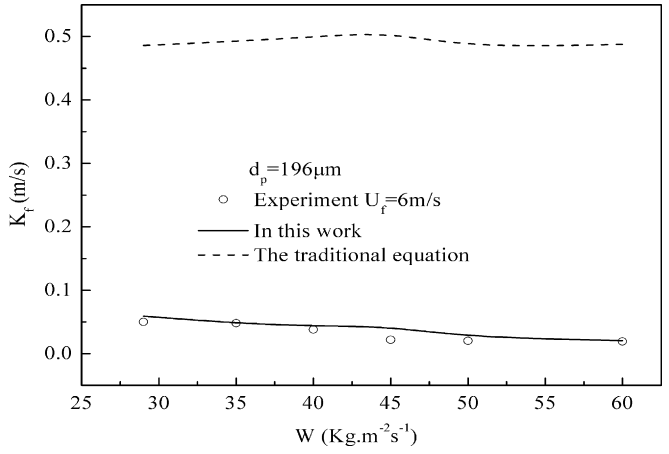

Fig. 9. Comparison of Subbarao's experimental data with theoretical predictions.

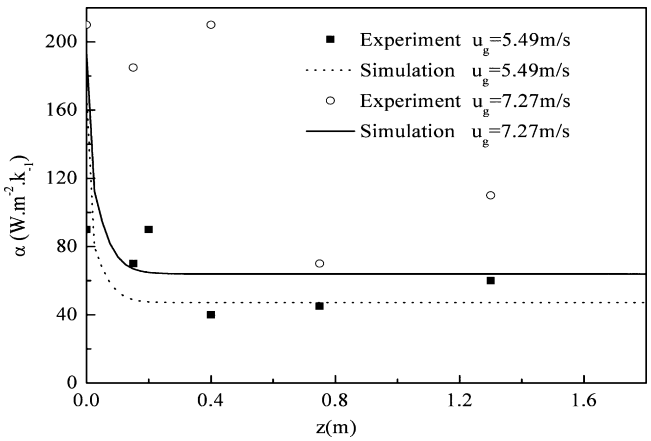

Fig. 10. Comparison of the experimental data and simulation results for the local coefficient of heat transfer.

7.3. Heat transfer

In order to verify the theoretical model for heat transfer based on the bed structure parameters in this work, the experimental data reported by Watanabe et al. [19] was employed to compare with the simulating results. In that experiment, the glass beads were firstly heated to 340 K, and then were employed to heat fluidizing air. The heat transfer between gas and solid has been measured in a high 1800 mm and internal diameter 21 mm fast fluidized bed. Other conditions of experiment and the method of solving have been described in detail in Appendix C. Fig. 10 shows the comparison of the experimental data and the simulation curves for the local heat transfer coefficient. In this figure, both the experimental data and the simulated heat transfer coefficient rapidly decrease from a high initial value near the bottom of the riser at each superficial gas velocity, beyond this region, however, it approaches a constant as bed height increases.

The experimental temperature profiles in the riser reported by Watanabe et al. [19] and the calculated temperature profiles by simulation in Fig. 11 suggest that with increase of the bed height, the gas temperature is quickly increased and reaches its asymptote, while the solid temperature decreases and reaches the same temperature as the gas. By comparing the experimental data and the simulation results, it can be found that the difference between the simulation and the experiment data for the gas temperature is

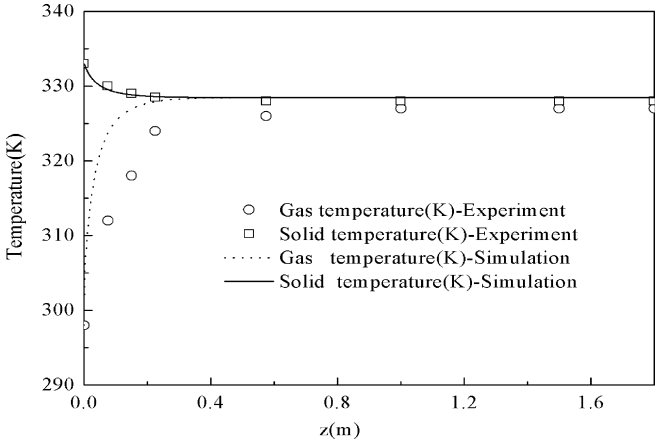

Fig. 11. Comparison between the experimental data and simulation results for the temperature profiles in the riser.

higher than that for solid temperature; this may be attributed to neglecting of the thermal conduction between gas and wall.

Like the mass transfer in the fast fluidized bed, the cluster plays an important role in heat transfer in the fast fluidized bed, Wang et al. [4] recently employed CFD to confirm this point of view. From Eq. (55), it can be see that the heat transfer coefficient is not only the function of heat transfer in every phase, but also the function of the temperature in every phase, so only using the traditional average method to predict this complex process is not appropriate.

8. Conclusions

There are significant effects of the heterogeneous gas–particles flow structure on the drag coefficient, the mass transfer coefficient and the heat transfer coefficient in fast fluidized beds. The following conclusions can be obtained:

1. The correlations from traditional average methods for these coefficients are not suitable to the heterogeneous gas–particles flow structure in fast fluidized beds.
2. Using the models developed considering the heterogeneous gas–particles flow structure, the momentum, mass and heat transfer coefficients can be more accurately predicted than the traditional average methods.
3. During the calculation of mass transfer and heat transfer, the effects of aggregating and dispersing of the particles on the mass and heat transfer coefficient can be neglected.

It is suggested that the present theory of calculating transfer coefficients based on the bed structural parameters in this work provides a kind of new tool for predicting the transfer behavior of fast fluidized bed. However, a great deal of experiment on gas–solid flow, inter-phase mass transfer and heat transfer still need to be conducted to verify and improve the applicability of the present theoretical analysis.

Notation

a_p specific surface area of particle (m^{-1})
a_c specific surface area of cluster (m^{-1})
c_c component concentration of gas in cluster phase (kg/m^3)
c_d component concentration of gas in dispersed phase (kg/m^3)
c_f averaged component concentration of gas (kg/m^3)
c_s component concentration of gas near the surface of particle (kg/m^3)
C_D drag coefficient
C_{Dc} drag coefficient in cluster phase
C_{Dd} drag coefficient in dispersed phase
C_{Di} drag coefficient between cluster and gas in dispersed phase
C_{D0} drag coefficient for single particle in gas flow
$\overline{C_D}$ averaged drag coefficient
C_p heat capacitivity of gas (J/(kg K))
D gas diffusion coefficient (m^2/s)
d_c diameter of cluster (m)
d_p diameter of particle (m)
F_D total drag force of flow gas on the particles in unit volume of gas–particles flow (N/m^3)
F_{Dc} drag force of flow gas on single particle in cluster phase (N)
F_{Dcn} drag force of flow gas in cluster phase on the particles in single cluster (N)
F_{Dcu} drag force of gas flow on particles in unit volume of cluster phase (N/m^3)
F_{Dd} drag force of flow gas on the single particle in dispersed phase (N)
F_{Di} drag force of flow gas in dispersed phase on the single cluster (N)
f volume friction of cluster phase
H heat quantity transferred from particles to gas in unit volume of the system ($J/(m^3\ s)$)
H_a heat quantity transferred from particles to gas due to aggregating and dispersing of the particles in unit volume of the system ($J/(m^3\ s)$)
H_c heat quantity transferred from particles in cluster phase to gas in cluster phase in unit volume of the system ($J/(m^3\ s)$)
H_d heat quantity transferred from particles in dispersed phase to gas in dispersed phase in unit volume of the system ($J/(m^3\ s)$)
H_i heat quantity transferred from particles on the surface of cluster to gas in dispersed phase in unit volume of the system ($J/(m^3\ s)$)
K coefficient of mass transfer between gas and particles cluster in homogeneous gas–particles system (m/s)
K_c coefficient of mass transfer between gas and particles in cluster phase (m/s)
K_d coefficient of mass transfer between gas and particles in dispersed phase (m/s)
K_f coefficient of mass transfer (m/s)
$\overline{K_f}$ averaged coefficient of mass transfer (m/s)
K_i coefficient of mass transfer between cluster and gas in dispersed phase (m/s)
M mass of naphthalene transferred from naphthalene particles to air flow in unit volume of the system ($kg/(m^3\ s)$)
M_a mass transferred from particles to air due to aggregating and dispersing of the particles in unit volume of the system ($kg/(m^3\ s)$)
M_c mass transferred from particles in cluster phase to air in cluster phase in unit volume of the system ($kg/(m^3\ s)$)
M_d mass transferred from particles in dispersed phase to air in dispersed phase in unit volume of the system ($kg/(m^3\ s)$)
M_i mass transferred from particles on the surface of clusters to air in dispersed phase in unit volume of the system ($kg/(m^3\ s)$)
Nu Nusselt number
Pr Prandtl number
Re_p Reynolds number for particle
Sc Schmidt number
Sh Sherwood number
t_f averaged temperature of gas (K)
t_{fc} temperature of gas in cluster phase (K)
t_{fd} temperature of gas in dispersed phase (K)
t_p averaged temperature of particles (K)
t_{pc} temperature of particles in cluster phase (K)
t_{pd} temperature of particles in dispersed phase (K)
U_f superficial gas velocity (m/s)
u_f gas velocity (m/s)
U_{fc} superficial gas velocity in cluster phase (m/s)
U_{fd} superficial gas velocity in dispersed phase (m/s)
U_p superficial particle velocity (m/s)
u_p particle velocity (m/s)
U_{pc} superficial particle velocity in cluster phase (m/s)
U_{pd} superficial particle velocity in dispersed phase (m/s)
U_s superficial slip velocity between gas and particles
U_{sc} superficial slip velocity between gas and particle in cluster phase (m/s)
U_{sd} superficial slip velocity between gas and particle in dispersed phase (m/s)
U_{si} superficial slip velocity between gas in dispersed phase and cluster (m/s)

Greek letters

α	coefficient of heat transfer between gas and particles cluster in homogeneous gas–particles system (J/(m^2 s K))
α_c	coefficient of heat transfer between gas and particles in cluster phase (J/(m^2 s K))
α_d	coefficient of heat transfer between gas and particles in dispersed phase (J/(m^2 s K))
α_f	coefficient of heat transfer (J/(m^2 s K))
$\overline{\alpha_f}$	averaged coefficient of heat transfer (J/(m^2 s K))
α_i	coefficient of heat transfer between cluster and gas in dispersed phase (J/(m^2 s K))
β_0	drag coefficient in a control volume (kg/m^3 s)
ε	voidage
ε_c	voidage in cluster phase
ε_d	voidage in dispersed phase
ε_f	averaged voidage
ε_i	voidage of inter-phase, i.e., the volume friction of gas except gas in clusters
λ	heat conductivity of gas (J/(m s K))
μ_f	viscosity of gas (kg/(m s))
ρ_f	density of gas (kg/m^3)
ρ_p	density of particle (kg/m^3)

Acknowledgements

The author is grateful to the support from National Natural Science Foundation of China under Grant No. 20736004, and from the State Key Development Program for Basic Research of China (973 Program) under Grant No. 2009CB219904.

Appendix A.

Simulation procedure for momentum transfer based on the bed structural parameters was established in this work. Gambit_2.2 was employed to generate the computational grid and Fluent 6.2.16 was used as the solver. The geometrical structure of fast fluidized bed employed in the experiment has been described in detail in Ref. [7]. In the calculating, at first, the bed structure parameters can be solved by EMMS [3] based on the averaged voidage and the velocity of gas and solid from CFD, thus the drag force in Eq. (18) can be obtained. The exchange coefficient of momentum between gas and solid can be calculated by Eq. (58).

In the fluidized bed, the solid phase has similar properties to a continuous fluid, so it often is treated as fluid phase. Therefore, the Eulerian model can be used to model the gas–solid fluidized bed reactors. In this model, the kinetic theory of granular flows is used. In this theory, the viscous forces and the solid pressure of the particulate phase can be described as a function of the so-called granular temperature. The governing equations in Eulerian notation are given in Table 1.

The differential equations in Table 1 can be solved by a finite volume method, These equations are discretized by the first-order upwind differencing scheme over the used finite volume. The popular SIMPLE algorithm by Patankar [21] is used to solve the pressure from the gas phase momentum equation, which requires a pressure correction equation that adjusts the pressure and the velocities after each iteration of discretized momentum equations. Each simulation is performed up to 20 s of real-time.

Inlet at the bed bottom is designated as velocity inlet boundary conditions for both the gas and solid phases. The boundary condition at the top of the bed is a pressure boundary fixed at the atmospheric pressure. Solids are leaved from the top due to drag force and then return to the computational domain from the bottom inlet with a same mass flux. Other boundary conditions are specified as wall, which are all set as no-slip wall boundary condition for both the gas and solid phases. The parameters of simulations have been described in Table 2.

Appendix B.

In this work, the experiment data reported by Subbarao and Gambhir [14] are employed. In that experiment, the air saturated with naphthalene is used as fluidizing gas, the 196 and 390 μm sand particles are fluidized in a fast fluidized bed of 2.5 cm I.D. and 105 cm in height, the process of naphthalene adsorbed by the solid is thought to be controlled by mass transfer between gases and solid and measured under the environmental condition. The mass transfer coefficient can be characterized by measuring the increasing weight of sand due to adsorbing the naphthalene in air. Other experimental detail may be found in Ref. [14]. For getting the

Table 1
Governing equations for two-fluid model and its constitutive relations.

Continuity equation ($k = g, s$)

$$\frac{\partial(\varepsilon_k\rho_k)}{\partial t} + \nabla(\varepsilon_k\rho_k u_k) = 0$$

$$\varepsilon_s + \varepsilon_g = 1$$

Momentum equation ($k = g, s$; $l = s, g$)

$$\frac{\partial(\varepsilon_k\rho_k u_k)}{\partial t} + \nabla(\varepsilon_k\rho_k u_k u_k) = -\varepsilon_k\nabla p_g + \varepsilon_k\rho_k g + \nabla\tau_k + \beta(u_l - u_k)$$

Gas phase stress

$$\tau_g = 2\mu_g S_g$$

Solid phase stress

$$\tau_s = [-p_s + \lambda_s\nabla\mu_s]\delta + 2\mu_s S_s$$

Deformation rate

$$S_k = \tfrac{1}{2}[\nabla u_k + (\nabla u_k)^T] - \tfrac{1}{3}\nabla u_k\delta$$

Solid phase pressure

$$p_s = \varepsilon_s\rho_s\Theta[1 + 2(1+e)\varepsilon_s g_0]$$

Solid phase shear viscosity

$$\mu_s = \tfrac{4}{3}\varepsilon_s^2\rho_s d_p g_0(1+e)\sqrt{\frac{\Theta}{\pi}} + \frac{2\mu_{s.dilute}}{(1+e)g_0}\left[1 + \tfrac{4}{5}(1+e)\varepsilon_s g_0\right]^2$$

$$\mu_{s.dilute} = \tfrac{5}{96}\rho_s d_p\sqrt{\pi\Theta}$$

Solid phase bulk viscosity

$$\lambda_s = \tfrac{4}{3}\varepsilon_s^2\rho_s d_p g_0(1+e)\sqrt{\frac{\Theta}{\pi}}$$

Radial distribution functions

$$g_0 = \left[1 - \left(\frac{\varepsilon_g}{\varepsilon_{sm}}\right)^{1/3}\right]^{-1}$$

Granular temperature equation

$$\tfrac{3}{2}\left[\frac{\partial(\varepsilon_s\rho_s\Theta)}{\partial t} + \nabla(\varepsilon_s\rho_s u_s\Theta)\right] = \tau_s : \nabla u_s - \nabla q - \gamma + \beta\overline{C_g C} - 3\beta\Theta$$

Collisional energy dissipation

$$\gamma = 3(1-e^2)\varepsilon_s^2\rho_s g_0\Theta\left[\frac{4}{d_p}\sqrt{\frac{\Theta}{\pi}} - \nabla u_s\right]$$

Flux of fluctuating energy

$$q = -k\nabla\Theta$$

Conductivity if the fluctuating energy

$$k = \frac{2k^k[1+(6/5)(1+e)\varepsilon_s g_0]^2}{(1+e)g_0} + k^c$$

$$k^k = \tfrac{75}{384}d_p\rho_s\sqrt{\Theta\pi}$$

$$k^c = 2\varepsilon_s^2\rho_s d_p g_0(1+e)\sqrt{\frac{\Theta}{\pi}}$$

Drag coefficient

Gidaspow et al. [13]

$\varepsilon_g \geq 0.8$:

$$\beta = \tfrac{3}{4}C_D\frac{\varepsilon_s\varepsilon_g\rho_g|u_g - u_s|}{d_p}\varepsilon_g^{-2.65}$$

$\varepsilon_g < 0.8$

$$\beta = 150\frac{\varepsilon_g\varepsilon_s\mu_g}{\varepsilon_g d_p^2} + 1.75\frac{\rho_g\varepsilon_s|u_g - u_s|}{d_p}$$

In this work

$$\beta_0 = \frac{\varepsilon_g^2}{|ug - us|}F_d$$

Table 2
Parameters setting for the simulation.

Particle diameter	54 μm
Particle density	930 kg/m^3
Grid size Δx	5 mm
Grid size Δy	40 mm
Riser height	10.5 m
Superficial gas velocity U_{g0}	1.52
Solids flux G_s	14.3
Initial bed height H_0	1.25
Coefficient of restitution	0.9
Time step	5.0e−5s
Unsteady formulation	First-order implicit
Pressure–velocity coupling	Phase coupled SIMPLE
Momentum discretization	First-order upwind
Max. number of iterations per time step	30
Convergence criteria	10e−3
Under relaxation factors	0.7 for pressure, 0.3 for momentum and 0.2 for volume and granular temperature
Maximum solid packing volume fraction	0.63

averaged mass transfer coefficient, a one-dimensional mass balance differential equation has to be developed. Based on the mass conversion, the active component of gas in the dispersed phase can be expressed as:

$$M_{outd} - M_{ind} = M_d + M_i + M_{dc} + M_a \tag{B-1}$$

where M_{dc} is the mass transferred from high concentration gas in the cluster to the low concentration gas in the dispersed phase by diffusion and seepage:

$$M_{dc} = AdzK_{dc}a_c f\varepsilon_c(c_c - c_d) \tag{B-2}$$

K_{dc} is the coefficient of mass exchange between lower concentration gas in the cluster phase and the higher concentration gas in the dispersed phase, and for the sphere particles, it can be expressed with the equation developed by Higbie [20]:

$$K_{dc} = 2.0\frac{D\varepsilon_c}{d_c} + \sqrt{\frac{4D\varepsilon_c}{\pi t_1}} \tag{B-3}$$

where t_1 is

$$t_1 = \frac{d_c}{|(U_{fc}/\varepsilon_c) - (U_{pc}/(1-\varepsilon_c))|} \tag{B-4}$$

Based on the principle of mass transfer [11], Eq. (B-1) is rewritten as:

$$\begin{aligned} U_{fd}(1-f)\frac{dc_d}{dz} &= K_d a_p(1-\varepsilon_d)(1-f)(c_{sd} - c_d) \\ &+ K_i a_c(1-\varepsilon_c)f(c_{si} - c_d) \\ &+ K_{dc}a_c f\varepsilon_c(c_c - c_d) + m_{ad} \end{aligned} \tag{B-5}$$

By the similar procedure, the mass conservation equation for the active component of gas in the cluster phase is derived as:

$$U_{fc}f\frac{dc_c}{dz} = K_c(a_p - a_c)(1-\varepsilon_c)f(c_{sc} - c_c) - K_{dc}a_c f\varepsilon_c(c_c - c_d) + m_{ac} \tag{B-6}$$

For a certain system with known initial and boundary conditions, the averaged mass transfer coefficient can be obtained by combining Eqs. (37), (38), (B-5) and (B-6).

Appendix C.

In this work, the experiment reported by Watanabe et al. [19] is employed to be simulated. In that experiment, the glass beads with the particle size 420–590 μm is employed, the circulation solid flux is 86.67–90.08 kg m^{-2} s^{-1}, the glass beads is firstly heated to 430 K and then be employed to heat the cold gas in the fast fluidized bed of 21 mm internal diameter and 1800 mm in height, the process of heat transfer between gas and solid is measured, and other experimental detail may be found in Ref. [19]. For getting the averaged heat transfer coefficient, a one-dimensional energy balance differential equation has to be developed to get the evolution of temperatures along the fluidized bed. However, because the glass beads are just heated to 340 K, the radiation heat transfer can be neglected. Thus, based on the conversion of energy, the heat transfer for gas in the dispersed phase is

$$H = H_i + H_d + H_{dc} + H_a \tag{C-1}$$

The flux of heat diffusion H_{dc} means that the flux of heat transferred from the high temperature gas in the cluster phase to the low temperature gas in the dispersed phase. It can be expressed as:

$$H_{dc} = Adz\alpha_{dc}a_c f\varepsilon_c(t_{fc} - t_{fd}) \tag{C-2}$$

where α_{dc} is the coefficient of heat exchange between the gas in dispersed phase and the gas in cluster phase. By the analogy with mass transfer and modifying the Higbie's formula [20], α_{dc} can be expressed as:

$$\alpha_{dc} = 2.0\frac{\lambda\varepsilon_c}{d_c} + 2\sqrt{\frac{\rho_f C_p \lambda\varepsilon_c}{\pi t_1}} \tag{C-3}$$

Eq. (C-1) can be rearranged to

$$\begin{aligned} \rho_f c_p U_{fd}(1-f)\frac{dt_{fd}}{dz} &= \alpha_d a_p(1-\varepsilon_d)(1-f)(t_{pd} - t_{fd}) \\ &+ \alpha_i a_c(1-\varepsilon_c)f(t_{pc} - t_{fd}) \\ &+ \alpha_{dc}a_c f\varepsilon_c(t_{fc} - t_{fd}) + h_a \end{aligned} \tag{C-4}$$

By using the same method with Eq. (C-1), the heat transfer equation for the solid in the dispersed phase and for gas and solid in the cluster phase can be derived, respectively. The heat transfer differential equation for solid in the dispersed phase is:

$$\rho_p c_s U_{pd}(1-f)\frac{dt_{pd}}{dz} = -\alpha_d a_p(1-\varepsilon_d)(1-f)(t_{pd} - t_{fd}) - h_a \tag{C-5}$$

The heat transfer differential equation for gas in the cluster phase is:

$$\rho_f c_p U_{fc} f\frac{dt_{fc}}{dz} = \alpha_c(a_p - a_c)f(1-\varepsilon_c)(t_{pc} - t_{fc}) - \alpha_{dc}a_c\varepsilon_c f(t_{fd} - t_{fc}) - h_a \tag{C-6}$$

The heat transfer differential equation for solid in the cluster phase can be expressed as:

$$\begin{aligned} \rho_p c_s U_{pc} f\frac{dt_{pc}}{dz} &= -\alpha_c(a_p - a_c)f(1-\varepsilon_c)(t_{pc} - t_{fc}) \\ &- \alpha_i a_c(1-\varepsilon_c)f(t_{pc} - t_{fd}) - h_a \end{aligned} \tag{C-7}$$

For a certain system with the initial and boundary conditions known, the averaged heat transfer coefficient can be solved by coupling Eqs. (53)–(55), (C-4), (C-5), (C-6) and (C-7).

References

[1] H. Li, Y. Xia, Y. Tung, M. Kwauk, Micro-visualization of clusters in fast fluidized bed, Powder Technol. 66 (3) (1991) 231–235.
[2] H. Schoenfelder, M. Kruse, J. Werther, Two-dimensional model for circulating fluidized-bed reactors, AIChE J. 42 (7) (1996) 1875–1888.

[3] N. Yang, W. Wang, W. Ge, et al., CFD simulation of concurrent-up gas–solid flow in circulating fluidized bed with structure-dependent Drag coefficient, Chem. Eng. J. 96 (1–3) (2003) 71–80.
[4] S.Y. Wang, L.J. Yin, H.L. Lu, L. Yu, B. Jacques, Z.H. Hao, Numerical analysis of interphase heat and mass transfer of cluster in a circulating fluidized bed, Powder Technol. 189 (1) (2009) 87–96.
[5] O. Bolland, R. Nicolai, Describing mass transfer in circulating fluidized beds by ozone decomposition, Chem. Eng. Commun. 187 (2001) 1–21.
[6] W. Dong, W. Wang, J. Li, A multiscale mass transfer model for gas–solid riser flows: Part 1—Sub-grid model and simple tests, Chem. Eng. Sci. 63 (2008) 2798–2810.
[7] J. Li, M. Kwauk, Particle-fluid Two-phase Flow: The Energy-Minimization Multi-scale Method, Metallurgical Industry Press, Beijing, 1994, pp. 23–40.
[8] C.Y. Wen, Y.H. Yu, Mechanics of fluidization, Chem. Eng. Prog., Symp. Ser. 62 (1966) 100–111.
[9] S. Ergun, Fluid flow through packed columns, Chem. Eng. Prog. 48 (1952) 89–94.
[10] K. Jung, R.D. La Nauze, Sherwood numbers for burning particles in fluidized beds, in: D. Kunii, S.S. Cole (Eds.), Fluidization IV, Engineering Foundation, New York, 1983, pp. 427–434.
[11] R.B. Bird, W.E. Stewart, E.N. Lightfoot, Transport Phenomena, John Wiley, New York, 1960.
[12] P.N. Rowe, K.T. Clayton, J.B. Lewis, Heat and mass transfer from a single sphere in an extensive flowing fluid, Trans. Inst. Chem. Eng. 43 (1965) 14–31.
[13] D. Gidaspow, R. Bezburuah, J. Ding, Hydrodynamics of circulating fluidized beds, kinetic theory approach, in: Fluidization VII, Proceedings of the 7th Engineering Foundation Conference on Fluidization, 1992, pp. 75–82.
[14] D. Subbarao, S. Gambhir, Gas particle mass transfer in risers, in: R. Grace, J. Zhu, H.de. Lasa (Eds.), Proceeding of the 7th International Conference on Circulating Fluidized Beds, Canadian Society for Chemical Engineering, Ottawa, Canada, 2002, pp. 97–104.
[15] R.W. Breault, C.P. Guenther, Mass transfer in the core-annular and fast fluidization flow regimes of a CFB, Powder Technol. 190 (3) (2009) 385–389.
[16] B.L. Yang, X.W. Zhou, X.H. Yang, C. Chen, L.Y. Wang, Multi-scale study on the secondary reactions of fluid catalytic cracking gasoline, AIChE J. 55 (8) (2009) 2138–2149.
[17] R.W. Breault, A review of gas–solid dispersion and mass transfer coefficient correlations in circulating fluidized beds, Powder Technol. 163 (1–2) (2006) 9–17.
[18] F. Scala, Mass transfer around freely moving active particles in the dense phase of a gas fluidized bed of inert particles, Chem. Eng. Sci. 62 (16) (2007) 4159–4176.
[19] T. Watanabe, M.Y.C. Hasatani, Y.S. Xie, I. Naruse, Gas–solid heat transfer in fast fluidized bed, in: P. Basu, M. Horio, M. Hasatani (Eds.), Proceeding of the 3rd International Conference on Circulating Fluidized Beds, PERGAMON Press, Oxford, 1991, pp. 283–288.
[20] R. Higbie, The rate of absorption of a pure gas into a still liquid during short period of exposure, Trans. Am. Inst. Chem. Eng. 31 (1935) 365–389.
[21] S.V. Patankar, Numerical Heat Transfer and Fluid Flow, Hemisphere Publishing Corp., 1980.